SME Annual Conference
Feb. 26 - Mar. 01, 2023, Denver, CO

Preprint 23-042

CONTRIBUTION OF INDIVIDUAL SUPPORT COMPONENTS TO ROOF STABILITY IN A LONGWALL GATEROAD

Z. Khademian, CDC NIOSH, Pittsburgh, PA
M. Sears, CDC NIOSH, Pittsburgh, PA
G. S. Esterhuizen, Independent Mining Engineer, Pittsburgh, PA

ABSTRACT

According to the 2010-2019 Mine Safety and Health Administration (MSHA) accident report database, 91% of reported ground control accidents in U.S. longwall mines were caused by roof instability. Gateroads are subject to significant changes in loading conditions from the development to the longwall abutment loading phases. When combined with thinly bedded shale roof, found in many U.S. longwall coal mines, the design of efficient roof support becomes challenging. In previous work, the Bonded Block Method (BBM) modeling of roof by UDEC was validated against field extensometer measurements in a longwall gateroad entry roof at a 180-m depth of cover. The BBM was shown as capable of capturing delamination and buckling of shale roof, one of the main roof instability mechanisms in longwall mines. This paper presents the recent findings on the roof-support interaction using BBM models of the same longwall entry. The effects of cable bolts, roof bolt density, and strap support on potential roof instability are studied. These types of studies are difficult and costly to conduct in an operating mine. Results show how the contribution of bolts, straps, and cable bolts can be quantified using the BBM models. The study demonstrates the potential for BBM numerical models to help understand the complex roof and support system interactions and to assist with optimizing gateroad support systems.

INTRODUCTION

The design of support systems for gateroad entries in U.S. longwall mines is mostly through local experience and in-mine trial and error that may lead to under-designed or over-designed support patterns. MSHA database shows that from 2010 to 2019, roof falls accounted for 91% of total reported ground control accidents in the US underground coal mines (Rashed, et al. 2022). One of the challenges in developing support design guidelines for entry roof in longwall mines is the variation of support performance with roof geology and stress patterns. The contribution of individual support elements is difficult to quantify in an operating mine because the support system is required to be fully functional at all times and removing certain supports to assess their contribution to stability is not prudent. In addition, local changes in the geology complicate the evaluation of the results of field trails. The National Institute for Occupational Safety and Health (NIOSH) has initiated a research project to evaluate methods for designing entry roof supports by collecting data on the roof geology and support systems in U.S. longwall mines, and conducting field instrumentations, laboratory testing, and numerical modeling. Numerical models allow a single support, geology, and loading parameters to be changed as part of a support study.

Numerical models validated against field data can be useful tools to examine the support performance under different geologic and stress conditions. However, the performance of conventional continuum modeling tools is inherently limited when the rock failure mechanism is mostly delamination and buckling of rock strata (Tulu et al., 2016 and Esterhuizen, 2012), two main mechanism governing roof instability in U.S. longwall mines (Hasenfus and Su, 2006). Esterhuizen et al. (2019) used a combined brittle/shear mechanism and realistically simulated the strength anisotropy and delamination of bedded strata in continuum models. However, discontinuum modeling techniques such as BBM are expected to be more effectively represent the mechanical response of rock and its interaction with the support systems.

While the majority of previous studies using BBM have focused on the laboratory-scale rock fracturing process, there has been some work on field-scale behavior of rock using BBM, such as modeling shear fracture propagation above coal mine entries (Coggan et al., 2012), the longwall caving process (Gao and Stead, 2014), and coal rib spalling (Sinha and Walton, 2021). For validating the BBM technique for studying longwall entry roof response, Khademian et al., (2021) evaluated the BBM technique using the Universal Distinct Element Code (UDEC). The authors constructed an entry-scale model of a longwall mine in West Virginia and validated the BBM modeling results against field measurements. This paper presents further work to evaluate the contribution of different support units to the stability of the entries using the validated BBM models. This series of studies aims to develop procedures for modeling supported entries and the surrounding rockmass that can be used to evaluate support alternatives under different geologic and stress conditions.

MODELING METHODOLOGY

The BBM technique in UDEC is used to model rock as an assembly of smaller blocks with triangular shapes (trigon), bonded together at their contacts with cohesion and tensile strengths. The so-called micro mechanical properties associated with trigons are the contacts' normal and shear stiffnesses, cohesion, and tensile strengths that together with the block material properties determine the macro mechanical response of the assembled rock unit. The blocks themselves were treated as elastic materials. A longwall mine in West Virginia was selected for evaluating support performance by the BBM technique. A detailed-scale model of the gateroad entry in the study mine was constructed and the micromechanical properties assigned to the trigon blocks were discussed previously (Khademian et al., 2022). The boundary conditions on the entry model after the development phase were obtained from field monitoring and panel-scale numerical modelling results in the study mine (Esterhuizen et al., 2019). The entry development was modeled by removing materials within the boundaries of the entry and then gradually releasing traction on the mined boundaries in ten decremental loading steps. The primary and secondary support system components were installed at the seventh step in the unloading process, assuming the 10th unloading step represents the completion of the entry development phase.

The abutment loading was extracted from the panel-scale model above the roof line at the corner of the tailgate entry. Then, the loading was applied to the boundary of the entry model in stages. The vertical loads were applied directly to the top of the model. The horizontal loading was gradually applied to the side of the model for each stage of mining using a displacement-controlled loading until the desired stress conditions were met at a location 3 m above the roof line. The modeled roof was considered failed when the roof slabs were accelerating (increasing velocity) under constant boundary loading conditions. Khademian et al., (2022) used this approach and showed that the displacement of different units in the roof after support installation are close to the extensometer measurements conducted in the study site.

DESCRIPTION OF MINE SITE

The research takes place in a longwall mine in West Virginia, mining the lower Kittanning coal bed with 152 m to 243 m of cover. The

width of the longwall panels is 365 m. The mining height is about 2.1 m with the entry development height up to 2.4 m. The width of the entry and crosscut developments is 5.5 m. The instrumentation site is in the tailgate of the third panel in the district under 180 m of cover and was part of a three-entry gateroad system as shown in Figure 1.

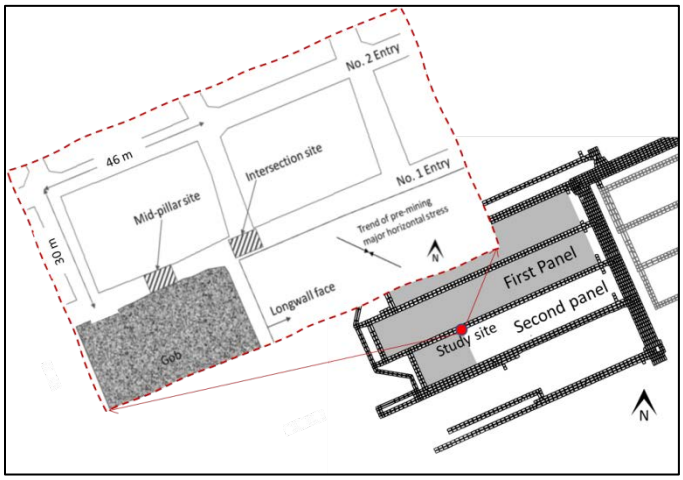

Figure 1. Pillar layout and monitoring site location at the longwall mine selected for this study.

Instrumentation and then monitoring were started a few days after development of the gateroad entries and continued until the second panel mine-by. Figure 1 shows the details of the mine layout and location of the instrumentation site on the last day of monitoring.

Geotechnical setting and instrumentation site

The overburden in the study mine consists of alternating sandstone and shale beds with sandstone layers between 9-m and 18-m thick. The thinly bedded shale above the Lower Kittanning coalbed ranges from dark gray to carbonaceous clay shale. The Johnstown limestone is located above this sandy zone. Table 1 lists the strength and mechanical properties of the rocks within the immediate roof. As shown by Esterhuizen et al. (2013), the Coal Mine Roof Rating (CMRR) (Molinda and Mark 1994) is used to estimate the large-scale field strength of the strata.

Table 1. Key rock properties at the study site.

Rock type	Elastic modulus (GPa)	Friction angle (degrees)	Cohesion (MPa)	Tensile strength (MPa)
Limestone	50	30	34	11
Gray clay shale	8	28	6	2
Clay shale	10	28	7	2
Carbonaceous shale	15	28	11	4
Shaley sandstone	18	38	10	3

The support performance was measured by load cells installed underneath the face plates of the cable bolts at the time of installation. The cable bolt load cells and roof extensometer were installed between 20 and 30 m outby the advancing heading. The roof sag was monitored by three 2.4-m-long extensometers (No. 1, No. 2, and No. 3 in Figure 4a) and one roof extensometer of 6 m length (No. 5 in Figure 4a).

Support system

The primary roof support in the study mine was rows of four fully grouted #6 bars with a 1.8 m height, spaced on 1.2-m centers. Fully grouted bolts were also installed at a 45-degree angle at the corner of the rib and roof, spaced on 2.4-m centers. The secondary support of the roof was a pair of cable bolts (3 m by 15 mm) installed through a strap every 2.4 m with 1.2 m of resin grout. Secondary support was installed about 18.2 to 30.4 m outby the advancing face. The standing support system was also used in the form of two rows of nine-point wooden cribs, but they are not considered in the models here because from crib load measuring devices, the standing supports did not take noticeable loads until after the second panel mined by.

NUMERICAL MODELING

In order to model thinly bedded rock units, trigons in the scale of centimeters should be constructed. For full-scale modeling of longwall mines, this level of detail leads to prohibitive computation time. One approach is to use sub-modeling where stress boundary conditions for an isolated area are obtained from a low-resolution (panel-scale) model and then are used to define the boundary conditions in a high-resolution (entry-scale) model as described in the following sections.

Entry loading condition by panel-scale model

Tulu et al. (2018) constructed a panel-scale model of the study site and validated the stress variation during mining against field measurements by Hollow Inclusion (HI) stress cells. The stress around the gateroad entries was used here to define the boundary condition of the entry-scale models. Stress distribution results from the panel-scale models at the end of the monitoring period with the actual longwall panel layout are shown in Figure 2.

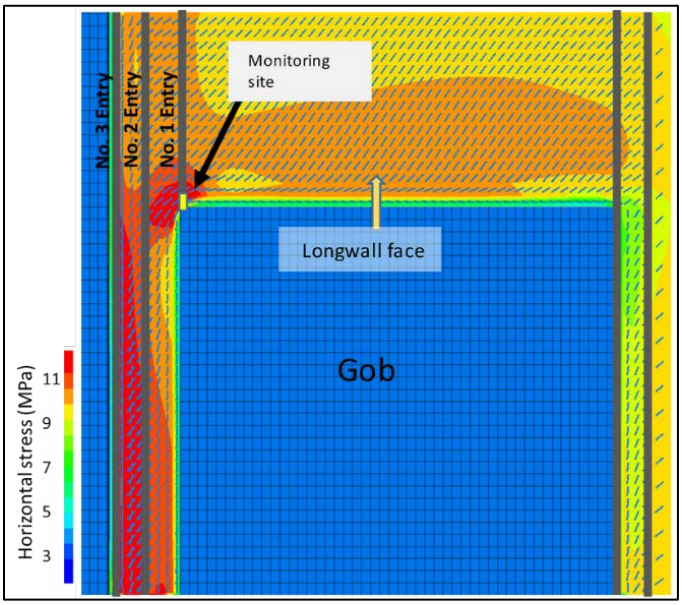

Figure 2. Maximum horizontal stress distribution and orientation 3 m above the mined coal bed in the panel-scale model (after Esterhuizen, et al. 2019).

Figure 3 shows the gateroad loading paths from the model recorded as the vertical and horizontal stresses at different mining stages, recorded 3 m above the roof line. In Figure 3, each marker on the curves shows a 9-m advance of the longwall face. The initial stress state in the model is with the horizontal stress of 7.1 MPa and vertical stress of 4.2 MPa. Compared to the other two entries, the stress path of the No. 1 (tailgate) entry shows a higher increase in horizontal stress. After the second panel mines by the monitoring site, stress at this location in the model reaches 12.8 and 12.7 MPa in horizontal and vertical directions, respectively. The change in stresses recorded by HI stress cells showed that 8 m above the tailgate roof, the vertical and horizontal stress values were 10.3 MPa and 11.5 MPa, respectively. With this validation, the stress path obtained from the model (Figure 3) at the tailgate entry (Entry No. 1) is applied as the boundary conditions of BBM entry-scale models described in the following section.

Entry-scale model of the site

Figure 4a shows the entry-scale model constructed for the study site, which is a two dimensional or a vertical slice through the entry No. 1. In total, 92 bedding planes in the roof and floor are modeled. Up to 11.5 m above the roof line, 65 slabs each 10 to 20 cm thick are modeled. BBM trigon blocks were generated up to 5 m above the roof line and the rest of the thinly bedded strata with no trigons.

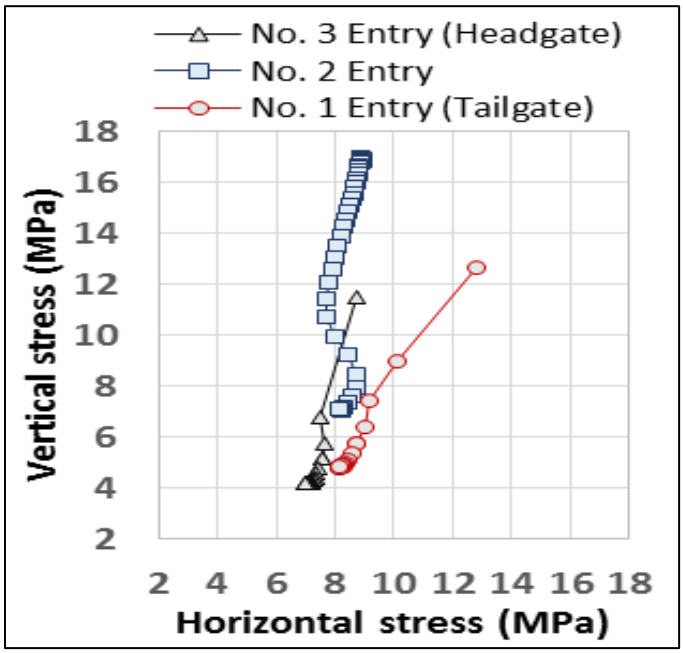

Figure 3. Stress path experienced by three entries in the model in vertical plane perpendicular to the long axis of the entry (Esterhuizen, et al. 2019).

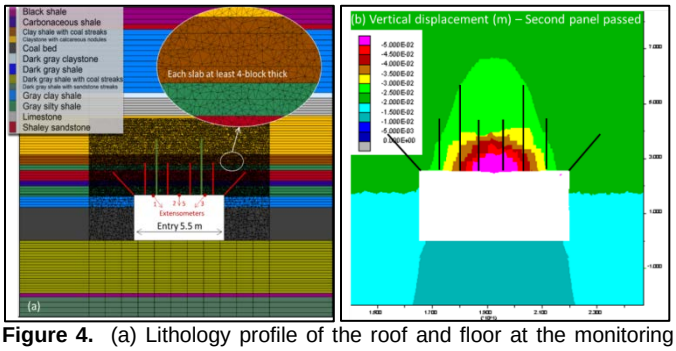

Figure 4. (a) Lithology profile of the roof and floor at the monitoring site along with the support system, and also trigons' geometry and density; (b) model results for vertical displacement after second panel mine-by (Khademian et al 2022).

The edge of trigons varies from 0.02 m to 0.06 m according to the thickness of each slab so that at least four trigons are located across each slab. The mine did not install rib bolts except at the pillar corners, indicating that rib spalling was not a concern during the longwall retreat. Thus, 3 m of ribs are constructed with relatively large trigons of 0.2 m edge to reduce computation time.

The modeling results from previous work is shown in Figure 4b, as the roof vertical displacement after the second panel mined by the instrumentation site. Figure 5a shows the roof vertical displacements at the left-hand and right-hand sides of the entry roof, confirming that the values predicted by the model are in agreement with the extensometer readings at the site. Figure 5b confirms the agreement between model and field measurements of the vertical displacements at the center of the roof. The validated model is considered as Case A and is used to study analyses of support system alternatives under similar conditions.

SUPPORT ALTERNATIVES

Calibration

The cable bolt response under mining-induced stresses is calibrated against the field measurements. Figure 6a shows the response of 8 cable bolts measured by the load cells versus the average roof sag measured by the extensometers. Most of the cable bolts were loaded between 50 to 100 kN when monitoring started, which was a few days after the bolt installation. This initial load can be associated with the thrust of the bolt machine during installation, and the displacement occurred after the installation. The peak load of individual bolts ranged from 190 to 320 kN with an average of 245 kN, which is close to the expected pick strength. The peak load for the cable bolts occurred between 60 to 90 mm of the roof sag. The average stiffness of the cable bolts from the slope of the curve between 16 and 70 mm of roof sag was 2.3 kN/mm, lower than the typical stiffness value measured during a controlled testing setup (Tadolini et al., 2012).

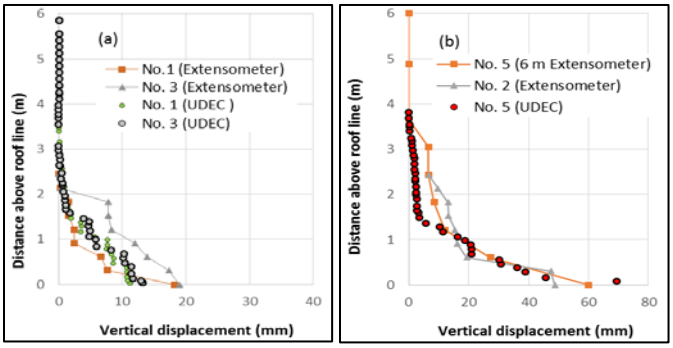

Figure 5. Vertical displacement above the roof line from model and field extensometers at (a) the No. 1 and No. 3 extensometer locations and (b) No. 2 and No. 5 extensometer locations shown in Figure 4. (Khademian et al 2022).

In an effort to calibrate the cable bolts under in-situ modeling conditions, the model in Figure 6b is used to conduct a pull-out test on one of the cable bolts in the roof. The bolt head is extended to include a block hanging from the roof with a thickness of 0.5 m. The block is pulled downwards and the load in the bolt is recorded versus the block displacement downwards. Through a trial-and-error approach, the cable and grout parameters are calibrated to match the average response of the cable bolts in Figure 6a. Figure 6c shows the force displacement curve of the cable bolt response after calibration.

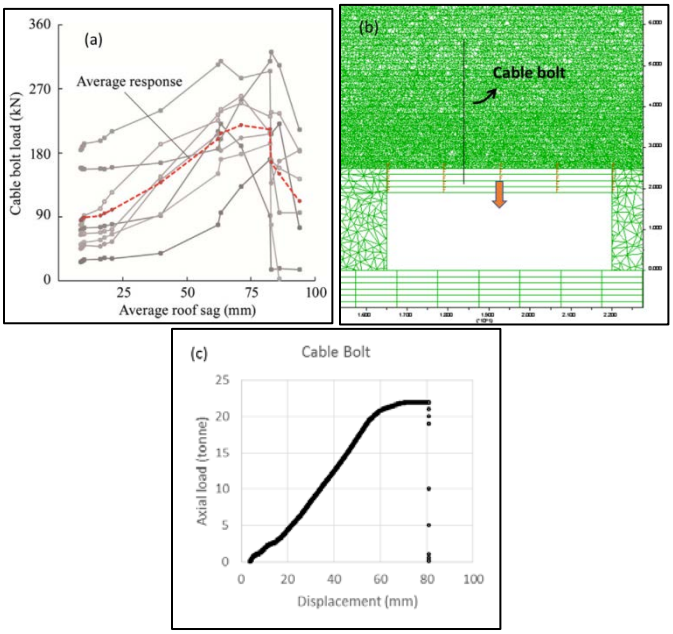

Figure 6. Cable bolts response measure in the field and respective model calibration. (a) Load cell results in 8 cable bolts instrumented in the field. (b) Model geometry for calibrating bolt mechanical parameters; and (c) Calibrated cable bolt response.

Besides the support systems installed in the mine with model results presented above, the effects of different support components on the roof are evaluated through studying four additional cases. Case #2 looks at the support performance without the strap through which

cable bolts were installed. Case #3 removes the 45-degree bolts from the support system. In addition to the 45-degree bolts, Case #4 removes the cable bolts and shows the major effects of cable bolts. Finally, Case #5 evaluates the roof response when the support is reduced by 0.3 m (1 ft) to 1.5-m-long bolts across the entry.

Case #2: Effects of strap support

As the first step, the effects of strap support on the roof stability are studied by removing the strap through which cable bolts are installed in the mine. The model is run according to the procedure in the modeling methodology section and is loaded through the full abutment loading sequence. Results of the model are shown in Figure 7a through 7d. Figure 7a shows the vertical displacement profile of the roof, showing that without the strap support, the roof layers became fragmented between bolts and the three first shale slabs (failure depth of 25 cm) spalled off between fully grouted bolts No 4 and 5. However, the roof remains stable as shown by the velocity plot in Figure 7b where the roof velocity remained close to zero. The horizontal stress profile shown in Figure 7c indicates the transfer of loads to the relatively stronger shale layer, 40-50 cm above the roof line. Figure 7d shows the maximum load in each of the bolts numbered from 1 to 8. Except for the B1 and B8 bolts that took minimal loads, the rest of the bolts have surpassed their yield strengths. The straps are demonstrated to provide local support to the immediate roof between the bolts, preventing the potential for injury by smaller rock fragments.

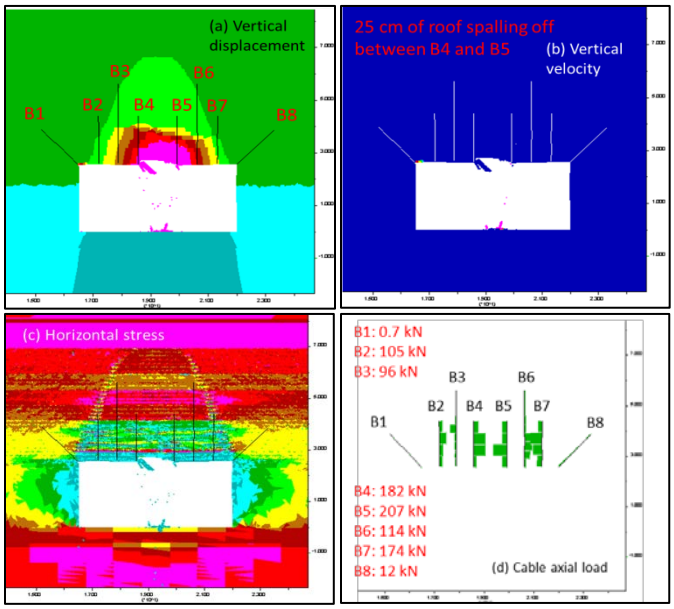

Figure 7. Model results showing entry response for Case #2 support system, assessing effects of strap. (a) vertical displacement (m); (b) vertical velocity (m/s); (c) horizontal stress (pa); (d) bolt axial load (kN).

Case #3: Effects of 45-degree bolts

From Case #2 observation, straps are shown to be useful for controlling local roof falls between bolts at the center of the entry. Also, it was shown that the 45-degree bolts (B1 and B8) seem to have little role in the roof control. To further evaluate B1 and B8 bolt performance, in Case #3, the model run is repeated without installing these two bolts. The results are shown in Figure 8a through 8d. From Figure 8a, the local roof spalling is limited to 10 cm above the roof line, but the overall displacement profile remains the same as that in Figure 7a. The roof remains stable as shown in Figure 8b. The horizontal stress is transferred to a stronger rock unit 60 to 80 cm above the roof line, 20 to 30 cm higher than that in the case with B1 and B8 bolts installed. From Figure 8d, the loads in the bolts stay similar to Case #2, showing that installing B1 and B8 bolts appears to have no significant effects on the roof stability. In fact, the lack of bolts B1 and B8 lead to the transfer of load higher in the roof with less skin damage. The B1 and B8 bolts are no longer installed at the case study mine after conducting an in-mine experiment prior to this study being conducted.

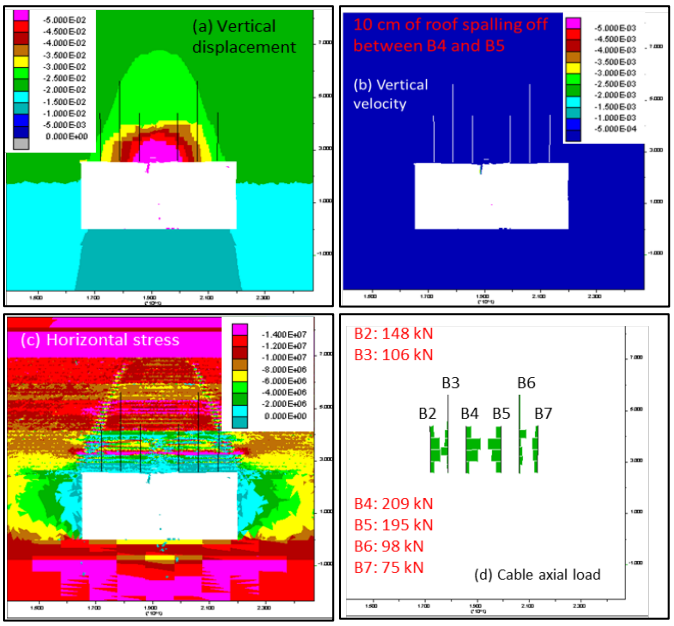

Figure 8. Model results showing entry response for Case #3 support system, assessing effects of 45-degree bolts. (a) vertical displacement (m); (b) vertical velocity (m/s); (c) horizontal stress (pa); (d) bolt axial load (kN).

Case #4: Effects of cable bolts

In Case #4, the performance of cable bolts is evaluated by removing them from the support system and repeating the model runs. The results are shown in Figure 9a through 9d. In Figure 9a, the roof is shown to be unstable. The velocity plots in Figure 9b shows that 60 cm of the roof will collapse. Loads are transferred to the layers above 90 cm in the roof but are mainly concentrated in 1.6 m above the roof in the strong shaley sandstone unit (Figure 9c). Segments of the bolts that are not broken yet take considerable load mainly because their last segment is 25 cm in the strong shaley sandstone, transferring the loads to the upper layers. Thus, in the next case, the length of the bolts are reduced so they are not within the strong shaley sand.

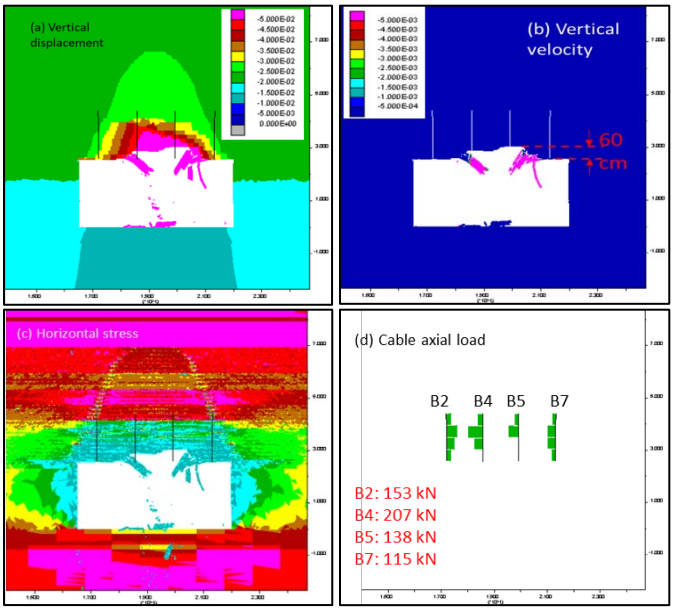

Figure 9. Modeling results for support system Case #3 for 5-ft long fully grouted bolts with no 45-degree bolts and no cable bolts. (a) vertical displacement (m); (b) vertical velocity (m/s); (c) horizontal stress (pa); (d) bolt axial load (kN).

Case #5: Effects of primary bolts

In the last step of the support performance evaluation, a minimal support layout is modeled by installing four fully grouted bolts with 1.5 m length (5 ft) evenly spaced across the entry. The difference with Case #4 is the reduction in the length of the primary bolts by 0.3 m (1 ft). The results are shown in Figure 10a through 10d.

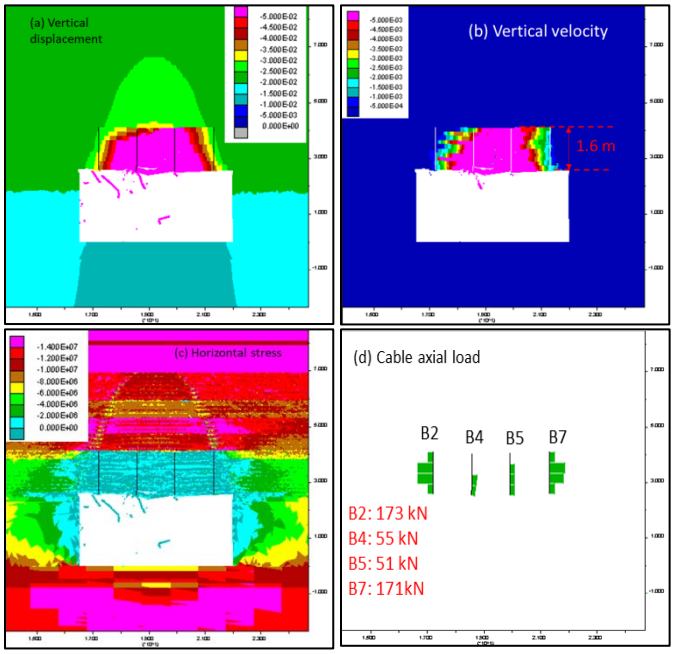

Figure 10. Modeling results for support system Case #4 for 4-ft long fully grouted bolts with no 45-degree bolts and no cable bolts. (a) vertical displacement (m); (b) vertical velocity (m/s); (c) horizontal stress (pa); (d) bolt axial load (kN).

Figure 10a shows significant roof movement up to 1.6 m above the roofline where the strong shaley sandstone unit is located. Figure 10b confirms the total collapse of the roof up to this depth. Figure 10c shows that the horizontal stress is close to zero and loads are transferred to the layer 1.6 m above the roof.

The results in Figure 9 and Figure 10 illustrate under-designed support systems that may lead to roof fall with a height of 0.6 and 1.6 m, respectively. The results demonstrate that the models agree with the judgement of the mine staff that four bolts are needed to provide adequate roof control for the longwall abutment loads and geologic conditions at the mine.

DISCUSSION

In the previous work (Khademian et al., 2022) in this series of papers, the application of BBM in evaluating the stability and failure mechanism of roof in longwall entries were evaluated. It was shown that the roof deformation predicted by the model agrees with the roof extensometer recordings in an instrumentation site in a longwall mine in West Virginia. In this work, we took one step further and evaluated the performance of alternative design layout and the roles of each component through a series of parametric tests. The results showed that cable bolts prevent the collapse of 0.6 m of roof. Changing the layout to rows of 1.5-m-long primary bolts leads to the collapse of roof with a height of 1.6 m. In contrast, the fully grouted 45-degree bolts appeared to have no significant effects for controlling the roof although might be useful for controlling cutters. Straps were shown to be effective in supporting 10 to 25 cm of the roof between the fully grouted primary bolts.

The application of boundary loads (Figure 3) to the entry-scale model (Figure 4b) from the global, panel-scale model (Figure 2) may need further improvements. Currently, vertical loads are applied as a single loading step for each stage of mining, according to Figure 3, while the horizontal stresses are applied using velocity-controlled loading in a gradual manner. The dynamic effects stemmed from the loading process should be minimized by a scheme that allows gradual application of vertical and horizontal loads. This improvement may affect the roof sagging and failure mechanism while changing the support response under quasi-static conditions.

CONCLUSION

The National Institute for Occupational Safety and Health (NIOSH) has initiated a research effort to evaluate methods for entry roof support design by collecting data on the roof geology and support systems in U.S. longwall mines, and conducting field instrumentations, laboratory testing, and numerical modeling. As a part of this effort, the Bonded Block Method (BBM) is being evaluated as a modeling tool to study and understand the roof failure mechanism and its interaction with alternative support systems. In this paper, a previously constructed and validated BBM model was used to study the effects of support system components in roof stability. Results show that the 45-degree fully grouted primary bolts have little to no effects on the stability of the roof. Models of support systems without straps showed 10-25 cm of local roof fall between primary bolts. Models with no cable bolts were shown 0.6 to 1.6 m of roof failure heights. These results will pave the way to further analyses on roof support performance under different roof geology and stress conditions.

REFERENCE

Coggan J., Gao F., Stead D., Elmo D. 2012. Numerical modelling of the effects of weak immediate roof lithology on coal mine roadway stability. Int J Coal Geol. 2012;90: 100–109.

Esterhuizen, G. S. 2012. "A stability factor for supported mine entries based on numerical model analysis." The 31st international conference on ground control in mining. Morgantown, WV: West Virginia University.

Esterhuizen, G.S., D. Gearhart, T. Klemetti, H. Dougherty, and M. Van Dyke. 2019. Analysis of gateroad stability at two longwall mines based on field monitoring results and numerical model analysis. International Journal of Mining Science and Technology 35-43.

Esterhuizen, G.S., T.S. Bajpayee, J.L. Ellenberger, and M.M. Murphy. 2013. Practical estimation of rock properties for modeling bedded coal mine strata using the Coal Mine Roof Rating. 47th US Rock Mechanics/Geomechanics Symposium. Alexandria, VA: American Rock Mechanics Association. 1634–1647.

Gao, F.Q., and D. Stead. 2014. The application of a modified Voronoi logic to brittle fracture modelling at the laboratory and field scale. International Journal of Rock Mechanics & Mining Sciences.

Hasenfus, G.J. and D.W.H. Su. 2006. Horizontal stress and coal mines: Twenty-five years of experience. International Conference on Ground Control in Mining. Morgantown, West Virginia University. 256-267.

Khademian, Z., Esterhuizen, G.S., Sears, M. 2022, Longwall Gateroad Stability Analysis Based on Field Monitoring and Bonded Block Modeling Results. In: Proceedings of the 41st International Conference on Ground Control in Mining." Canonsburg, PA.

Molinda, G.M. and C. Mark. 1994. Coal Mine Roof Rating (CMRR): A Practical Rock Mass Classification for Coal Mines. Information Circular 9387. U.S. Department of the Interior, Bureau of Mines.

Rashed, G., Y. Xue, Z. Khademian, and M. Sears. 2022. Ground-fall Accident Trends in Mining: 2010 to 2019. Mining, Metallurgy & Exploration.

Sinha S., Walton G. 2021. Modeling the behavior of a coal pillar rib using Bonded Block Models with emphasis on ground-support interaction. International Journal of Rock Mechanics and Mining Sciences. 2021; 148.

Tadolini C.S., Tinsly J., McDonnell J.P. The next generation of cable bolts for improved ground control. In: Proceedings of the 31st

International Conference on Ground Control in Mining, ICGCM. Morgantown, WV: West Virginia University; 2012. p. 27–34.

Tulu, I.B., G.S. Esterhuizen, D. Gearhart, T.M. Klemetti, K M. Mohamed, and D.W.H. Su. 2018. Analysis of global and local stress changes in a longwall gateroad." International Journal of Mining Science and Technology 127-135.

Tulu, I.B., G.S. Esterhuizen, T. Klemetti, M.M. Murphy, J. Sumner, and M. Sloan. 2016. A case study of multi-seam coal mine entry stability analysis with strength reduction method. International Journal of Mining Science and Technology, 193-198.